ORIGINAL ARTICLE

WILEY Cancer Science

Therapeutic efficacy evaluation of radioimmunotherapy with ^{90}Y-labeled anti-podoplanin antibody NZ-12 for mesothelioma

Hitomi Sudo[1] | Atsushi B. Tsuji[1] (iD) | Aya Sugyo[1] | Tsuneo Saga[2] (iD) | Mika K. Kaneko[3] | Yukinari Kato[3,4] (iD) | Tatsuya Higashi[1]

[1]Department of Molecular Imaging and Theranostics, National Institute of Radiological Sciences, National Institutes for Quantum and Radiological Science and Technology (QST-NIRS), Chiba, Japan

[2]Department of Diagnostic Radiology, Kyoto University Hospital, Kyoto, Japan

[3]Department of Antibody Drug Development, Tohoku University Graduate School of Medicine, Sendai, Miyagi, Japan

[4]New Industry Creation Hatchery Center, Tohoku University, Sendai, Miyagi, Japan

Correspondence
Atsushi B. Tsuji, Department of Molecular Imaging and Theranostics, National Institute of Radiological Sciences, National Institutes for Quantum and Radiological Science and Technology (QST-NIRS), Chiba, Japan.
Email: tsuji.atsushi@qst.go.jp

Podoplanin is a type I transmembrane sialomucin-like glycoprotein that is highly expressed in malignant mesothelioma. The rat-human chimeric antibody NZ-12 has high affinity for human podoplanin and antibody-dependent cellular cytotoxicity and is applicable for radioimmunotherapy (RIT) to enhance the antitumor effect. In the present study, we evaluated the in vivo and in vitro properties of radiolabeled NZ-12 and the antitumor effect of RIT with ^{90}Y-labeled NZ-12 in an NCI-H226 (H226) malignant mesothelioma xenograft mouse model. ^{111}In-labeled NZ-12 bound specifically to H226 cells with high affinity, and accumulation was high in H226 tumors but low in major organs. RIT with ^{90}Y-labeled NZ-12 significantly suppressed tumor growth and prolonged survival without body weight loss and obvious adverse effects. Higher podoplanin expression levels were observed in human mesothelioma specimens, suggesting higher tumor accumulation of ^{90}Y-labeled NZ-12 in patients compared with the H226 tumor xenografts. Our findings suggest that ^{90}Y-labeled NZ-12 is a promising RIT agent as a new therapeutic option for malignant mesothelioma that warrants further clinical studies to evaluate the dosimetry and efficacy in patients.

KEYWORDS
antibody, malignant mesothelioma, podoplanin, radiation, radioimmunotherapy

1 | INTRODUCTION

Malignant mesothelioma is an aggressive tumor with a poor prognosis[1] that is classified into three main types based on the histological features: epithelioid, sarcomatoid, and mixed.[2] Median overall survival in patients with malignant mesothelioma is 7 months.[3] Surgical resection may be offered to patients with early-stage disease, and systemic chemotherapy is the main treatment for patients with advanced-stage disease.[4,5] Most malignant mesothelioma patients receive chemotherapy, however, because the disease is often diagnosed at the advanced stage.[5] Although newly developed molecular-targeted drugs are expected to improve patient prognosis, current combination chemotherapy using pemetrexed and cisplatin is reported to prolong the overall survival by only 2.8 months compared with cisplatin alone.[4] Thus, more effective treatments are needed to improve the prognosis. Radioimmunotherapy (RIT) using radiolabeled monoclonal antibodies against tumor-associated antigens is a selective internal radiation therapy.[6] Several preclinical studies demonstrated promising therapeutic outcomes of RIT for solid tumors, including small cell lung cancer,[7,8] pancreatic cancer,[9,10]

and breast cancer.[11] RIT with antibodies recognizing antigens expressed on mesothelioma cells is a potential therapeutic option for malignant mesothelioma.

Podoplanin is a transmembrane sialomucin-like glycoprotein that is highly expressed in several types of cancer, such as brain tumor,[12] squamous cell carcinoma,[13-15] soft tissue tumors,[16] bladder cancer,[17] and malignant mesothelioma.[18,19] Podoplanin is associated with epithelial mesenchymal transition, migration, invasion, and metastasis,[20,21] and its expression correlates with the malignancy grade in brain tumors, lung cancer, and oral cancer.[21-23] Several anti-podoplanin antibodies inhibit cancer metastasis[24] and cancer progression[12,19] in mouse tumor models. Therefore, podoplanin is a promising therapeutic target in various cancers, including malignant mesothelioma.

Podoplanin expression is high in cancerous tissues, whereas expression is low in several normal tissues, such as kidney podocytes,[25] alveolar type I cells,[26] lymphatic endothelial cells,[27] basal epidermal keratinocytes,[15] and mesothelial cells.[28] The physiological expression of podoplanin in normal tissues raises some concern about the possible risks of toxicity to these normal tissues induced by podoplanin-targeted anticancer therapy. To address this concern, it is important to select an antibody that recognizes podoplanin expressed on cancer cells only and not on normal cells. We developed a rat anti-podoplanin monoclonal antibody, NZ-1, which has the above-mentioned property,[29] and converted it to a rat-human chimeric antibody named NZ-12.[30] These antibodies recognize podoplanin expressed on the surface of cancer cells, such as brain tumor, lung cancer, and malignant mesothelioma, but not in benign tumor cells or normal organs.[19,31] Therefore, NZ-12 has potential application for selective antitumor therapy including RIT against malignant mesothelioma.

In the present study, NZ-12 was labeled with radionuclides In-111 and Y-90 to evaluate the in vitro and in vivo properties as a theranostic pair. Y-90 is a pure beta emitter with a high energy level (maximum energy, 2.3 MeV) and an appropriate half-life (64.1 hours) for RIT using IgG.[32] In-111, a gamma emitter with 171 keV and 245 keV and a half-life of 67.4 hours, is used for diagnostic imaging and dosimetry as a surrogate for Y-90.[33,34] The combination of In-111 and Y-90 is used in clinical practice (eg, Zevalin)[34] in which the ^{111}In-labeled anti-CD20 antibody is used for patient selection by SPECT/CT imaging and the ^{90}Y-labeled anti-CD20 antibody is used for RIT of non-Hodgkin's lymphoma. In the present study, ^{111}In-labeled NZ-12 was used for biodistribution and dosimetry studies, and ^{90}Y-labeled NZ-12 was used to evaluate the antitumor effects in a mesothelioma mouse model.

2 | MATERIALS AND METHODS

2.1 | Antibodies

A rat-human chimeric antihuman podoplanin antibody, NZ-12,[30] and a mouse antihuman podoplanin antibody, LpMab-17,[35] were previously developed. As a control, human $IgG_{1\lambda}$ was purchased from Sigma-Aldrich (St Louis, MO, USA).

2.2 | Cell culture

Mesothelioma cell lines, NCI-H226 (H226, CRL-5826) and MSTO-211H (211H, CRL-2081), were obtained from ATCC (Manassas, VA, USA). The cells were cultured in RPMI-1640 (Wako Pure Chemical Industries, Tokyo, Japan) containing 10% FBS (Life Technologies, Carlsbad, CA, USA) in 5% CO_2 at 37°C.

2.3 | Immunofluorescence staining in vitro

H226 and 211H cells were seeded on coverslips, incubated overnight, and fixed with 4% paraformaldehyde the next day. Immunofluorescence staining was conducted using anti-podoplanin antibody LpMab-17 as a primary antibody with an Alexa Fluor 594 goat antimouse antibody (Molecular Probes, Eugene, OR, USA) as a secondary antibody. Coverslips were placed on glass slides using mounting medium with DAPI (Vector Laboratories, Burlingame, CA, USA). Fluorescence images were captured with an exposure time of 50 ms for podoplanin and 25 ms for DAPI using a fluorescence microscope BX53 (Olympus, Tokyo, Japan) and cellSens Standard software (ver. 1.7.1; Olympus).

2.4 | Radiolabeling of antibody

Antibodies were conjugated with p-SCN-Bn-CHX-A''-DTPA (CHX-A''-DTPA; Macrocyclics, Dallas, TX, USA) as described previously.[36] Briefly, the antibody (5 mg/mL) was reacted with an equal molar amount of CHX-A''-DTPA in 50 mmol/L borate buffer (pH 8.5) for 16 hours at 37°C. Conjugation ratio of CHX-A''-DTPA to antibody was estimated to be approximately 0.8 as determined by cellulose acetate electrophoresis. The CHX-A''-DTPA-conjugated antibody was purified by elution with 0.1 mol/L acetate buffer (pH 6.0) using a Sephadex G-50 (GE Healthcare, Little Chalfont, UK) column. $^{111}InCl_3$ (Nihon Medi-Physics, Tokyo, Japan) or $^{90}YCl_3$ (Eckert & Ziegler Radiopharma, Berlin, Germany) was incubated in 0.5 mol/L acetate buffer (pH 6.0) for 5 minutes at room temperature. Each was mixed with the CHX-A''-DTPA-antibody conjugate and incubated for 30 minutes at room temperature. The radiolabeled antibody was eluted with 0.1 mol/L acetate buffer (pH 6.0) using a Sephadex G-50 column for purification. Specific activity of ^{111}In-labeled NZ-12, ^{111}In-labeled control antibody, ^{90}Y-labeled NZ-12, and ^{90}Y-labeled control antibody was approximately 30, 40, 1100, and 800 kBq/μg, respectively. Radiochemical yields were approximately 60% for ^{111}In labeling and 35% to 50% for ^{90}Y labeling, and radiochemical purities were more than 95% after purification with a Sephadex G-50 column.

2.5 | Cell binding and competitive inhibition assays

For cell-binding assays, H226 and 211H cells (5.0×10^6, 2.6×10^6, 1.3×10^6, 6.3×10^5, 3.1×10^5, 1.6×10^5, 7.8×10^4, and 3.9×10^4) in PBS with 1% BSA (Sigma-Aldrich) were incubated with ^{111}In-labeled NZ-12 or control antibody on ice for 60 minutes. After washing, cell-bound radioactivity was measured using a gamma-counter (ARC-370M; Aloka, Tokyo, Japan). For competitive inhibition assays, H226 cells (2.0×10^6) in PBS with

1% BSA were incubated with ^{111}In-labeled NZ-12 in the presence of varying concentrations of intact NZ-12, CHX-A″-DTPA-conjugated NZ-12, or intact control antibody (0, 0.5, 0.9, 1.9, 3.8, 7.6, 15.2, and 30.3 nmol/L) on ice for 60 minutes. After washing, cell-bound radioactivity was measured with a gamma-counter. The dissociation constant was estimated by applying data to a one-site competitive binding model using GraphPad Prism software (ver. 7.0d, GraphPad Software, La Jolla, CA, USA).

2.6 | Tumor model

The animal experimental protocol was approved by the Animal Care and Use Committee of the National Institute of Radiological Sciences (13-1022, 26 May 2016), and all animal experiments were conducted in accordance with the Guidelines regarding Animal Care and Handling. H226 cells (3.5×10^6) were s.c. inoculated into male nude mice (BALB/c-nu/nu, 6 weeks old; CLEA Japan, Tokyo, Japan) under isoflurane anesthesia.

2.7 | Biodistribution of ^{111}In-labeled antibody

When H226 tumor volumes reached approximately 80 mm^3, mice (n = 5/time-point), were i.v. injected with 37 kBq of ^{111}In-labeled NZ-12 or ^{111}In-labeled IgG$_{1\lambda}$ in a total of 20 μg antibody adjusted by adding the appropriate amount of unlabeled antibody. The mice were killed by isoflurane inhalation at 1 hour, and at 1, 2, 4, and 7 days after injection. Blood, tumor, and organs of interest were sampled and weighed, and the radioactivity was measured using a gamma-counter. The uptake is represented as the percentage of injected radioactivity dose per gram of tissue (% ID/g). The absorbed dose of ^{90}Y-labeled antibody was estimated using the area under the curve based on the biodistribution data of ^{111}In-labeled antibody and the mean energy emitted per transition of Y-90,[37] 1.495×10^{-13} Gy kg (Bq s)$^{-1}$ as described previously.[7]

2.8 | Radioimmunotherapy with ^{90}Y-labeled antibody

When H226 tumor volumes reached approximately 80 mm^3, the mice were i.v. injected with intact NZ-12, ^{90}Y-labeled NZ-12 antibody (1.85, and 3.70 MBq, n = 10/dose) or ^{90}Y-labeled control antibody (3.70 MBq, n = 10) in a total of 20 μg antibody adjusted by adding the corresponding unlabeled antibody. Tumor size and body weight were measured at least twice a week for 8 weeks after dosing. Tumor size was measured using a digital caliper, and tumor volume was calculated using the following formula: tumor volume (mm^3) = (length × width^2)/2. When the tumor volume reached greater than 800 mm^3, the mouse was killed humanely by isoflurane inhalation.

2.9 | Histological analysis

H226 tumors were resected from mice on days 1, 3, and 7 after injection with 3.70 MBq of ^{90}Y-labeled NZ-12 and 3.70 MBq of ^{90}Y-labeled control antibody (n = 3/time-point). The tumors were fixed in 10% neutral-buffered formalin and embedded in paraffin. Tumor sections (1-μm thick) were deparaffinized and stained with hematoxylin and eosin. Tumor cell proliferation was evaluated by immunohistochemical staining with a rabbit anti-Ki-67 antibody (SP6; Abcam, Cambridge, MA, USA) and an antirabbit HRP/DAB Detection kit (Abcam) according to the manufacturer's instructions. Ki-67 index was calculated by counting the percentage of Ki-67-positive tumor cells per >2500 tumor cells in a section with 200× magnification (n = 3). Apoptosis was detected using the DeadEnd Colorimetric TUNEL System (Promega, Madison, WI, USA). A tissue array containing 19 cases of human malignant mesothelioma tissues (13 cases of epithelioid-type, three cases of sarcomatoid-type, and three cases of mixed-type) was obtained from Biomax (Rockville, MD, USA). The tissues were stained with 4 μg/mL of an anti-podoplanin antibody LpMab-17 and an Envision+ system (Agilent Technologies, Santa Clara, CA, USA). The nuclei were counterstained with hematoxylin.

2.10 | External-beam radiation with X-rays

When H226 tumor volumes reached approximately 80 mm^3, tumors (n = 5/dose) were irradiated with 0, 25, and 50 Gy of X-rays at a rate of 4.0 Gy/min using a TITAN-320 X-ray generator (Shimadzu, Kyoto, Japan). Other parts of the mouse body were covered with a brass shield to limit unnecessary radiation exposure. Tumor size and body weight were measured at least twice a week for 8 weeks after irradiation, and tumor volume was calculated using the formula mentioned above. When the tumor volume reached greater than 800 mm^3, the mouse was killed humanely by isoflurane inhalation.

2.11 | Statistical analysis

Data were analyzed by ANOVA with Dunnett's multiple comparison tests. Log-rank tests were used to evaluate Kaplan-Meier survival curves based on the endpoint of tumor volume of 500 mm^3. Data are expressed as means ± standard deviation (SD). The criterion of statistical significance was $P < .05$.

3 | RESULTS

3.1 | Podoplanin expression analysis in H226 and 211H cells

Two mesothelioma cell lines, H226 (podoplanin-positive) and 211H (podoplanin-negative), were used in the present study.[19] To confirm podoplanin expression in these cells, they were immunofluorescently stained with an anti-podoplanin antibody LpMab-17. Strong staining intensity was observed on the cell membranes of H226 cells, but not on 211H (Figure 1).

3.2 | In vitro characterization of antibody

In cell binding assays with H226 and 211H cells, ^{111}In-labeled NZ-12 bound to H226 cells with a maximum value of 34.5% ± 1.0% at 1×10^7 cells, whereas it did not bind to 211H cells (Figure 2A). ^{111}In-labeled human IgG$_{1\lambda}$ as an isotype-matched control did not bind to H226 cells (Figure 2B). From the competitive inhibition assay with H226 cells, the

dissociation constants of intact NZ-12 and CHX-A''-DTPA-conjugated NZ-12 were estimated to be 1.1 and 3.0 nmol/L, respectively (Figure 2C), suggesting that the loss of affinity by the chelate conjugation procedure was very limited. The control antibody $IgG_{1\lambda}$ did not inhibit the binding of ^{111}In-labeled NZ-12 to H226 cells (Figure 2D). Thus, CHX-A''-DTPA-conjugated NZ-12 was considered acceptable for the following in vivo experiments, and the human $IgG_{1\lambda}$ was used as a control.

3.3 | Biodistribution of ^{111}In-labeled antibody in nude mice bearing H226 tumors

Tumor uptake of ^{111}In-labeled NZ-12 and control antibody was similar at 1 hour after injection ($2.1 \pm 0.3\%$ ID/g of ^{111}In-labeled NZ-12 and $1.8 \pm 0.9\%$ ID/g of ^{111}In-labeled control antibody) shown in Table 1. Subsequently, ^{111}In-labeled NZ-12 tumor uptake significantly increased over time and reached $23.2 \pm 0.9\%$ ID/g on day 7, whereas the ^{111}In-labeled control antibody showed a slight increase and ranged from $6.5 \pm 0.5\%$ to $9.0 \pm 1.9\%$ ID/g (Table 1). On days 1, 2, 4, and 7, tumor uptake was significantly different between ^{111}In-labeled NZ-12 and control antibody ($P < .01$, Table 1). Biodistribution of ^{111}In-labeled NZ-12 in normal organs was almost similar to that of ^{111}In-labeled control antibody, although there were some statistically significant differences in blood, liver, spleen, and muscle ($P < .01$ or $P < .05$, Table 1). Based on these results, the absorbed dose was estimated when In-111 was replaced with Y-90. The dose absorbed by H226 tumors was 24.8 and 10.6 Gy when injected with 3.70 MBq of ^{90}Y-labeled NZ-12 and ^{90}Y-labeled control antibody,

respectively (Table 2). Among the absorbed doses in major organs, the highest values were observed in the lungs, 14.4 Gy for ^{90}Y-labeled NZ-12 and 15.9 Gy for ^{90}Y-labeled control antibody (Table 2).

3.4 | Treatment effects of ^{90}Y-labeled antibody in nude mice bearing H226 tumors

Giving 3.70 MBq of ^{90}Y-labeled NZ-12 significantly suppressed H226 tumor growth during the first 21 days compared with intact NZ-12 (0 MBq) and, thereafter, the tumor volumes gradually increased ($P < .01$, Figure 3A,B). In contrast, no significant tumor suppression was observed in the groups given 1.85 MBq of ^{90}Y-labeled NZ-12 and 3.70 MBq of ^{90}Y-labeled control antibody compared with intact NZ-12 (0 MBq) shown in Figure 3A. Kaplan-Meier survival curves based on the endpoint of tumor volume of 500 mm[3] are shown in Figure 3C. Giving 3.70 MBq of ^{90}Y-labeled NZ-12 induced significant survival prolongation compared with the other groups ($P < .01$ vs 0 MBq and 1.85 MBq of ^{90}Y-labeled NZ-12, and $P < .05$ vs 3.70 MBq of ^{90}Y-labeled control antibody), whereas survival did not differ among the groups given 0 MBq and 1.85 MBq of ^{90}Y-labeled NZ-12 and 3.70 MBq of ^{90}Y-labeled control antibody (Figure 3C). ^{90}Y-labeled NZ-12 treatment induced no significant body weight reduction compared with the 0-MBq group, whereas giving 3.70 MBq of ^{90}Y-labeled control antibody induced transient but significant body weight loss during the first 7 days ($P < .05$, Figure 3D).

3.5 | Histological analysis of H226 tumors treated with ^{90}Y-labeled NZ-12

Hematoxylin and eosin staining showed no marked histological changes in H226 tumors treated with intact NZ-12 (0 MBq), as shown in Figure 4. Sections of H226 tumors treated with 3.70 MBq of ^{90}Y-labeled NZ-12 showed a few small necrotic foci on days 1 and 3, and expansion of the necrotic area and hemorrhage were observed on day 7, in contrast to untreated tumors and tumors treated with intact NZ-12 (0 MBq) shown in Figure 4. Next, to evaluate the effects on cell proliferation, Ki-67-immunostaining was conducted. Cell proliferation did not change significantly in tumors treated with intact NZ-12 (0 MBq), whereas 3.70 MBq of ^{90}Y-labeled NZ-12 reduced cell proliferation (Ki-67-positive cells) in a time-dependent way (Figure 5), and the reduction was statistically significant on days 3 and 7 compared with untreated tumors and tumors treated with intact NZ-12 (0 MBq). In contrast, few apoptotic cells, as determined by TUNEL staining, were observed in any of the groups (data not shown).

3.6 | Podoplanin expression in human malignant mesothelioma specimens

Human malignant mesothelioma specimens containing three main histological types, epithelioid, sarcomatoid, and mixed, were immunostained with an anti-podoplanin antibody LpMab-17. A positive staining signal was observed both in the cytoplasm and in plasma membranes of tumor cells and tended to be stronger compared with H226 tumors (Figure 6). Table 3 provides a summary of the immunohistochemical staining data.
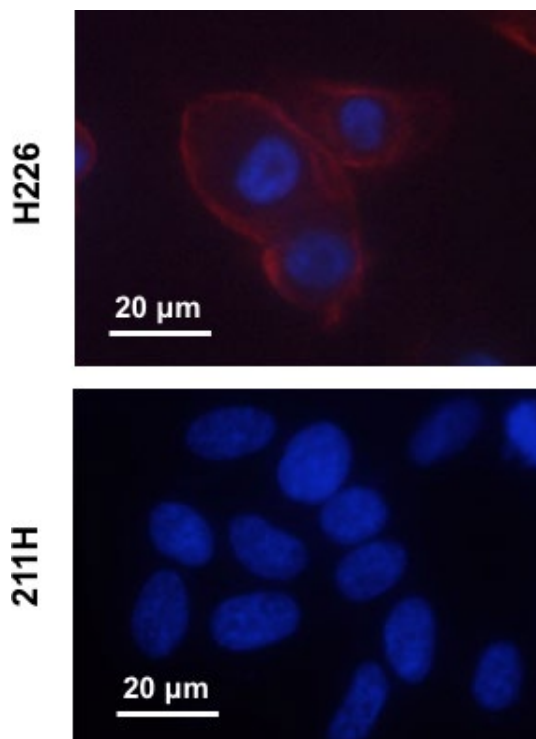

FIGURE 1 Immunofluorescence staining of H226 (podoplanin-positive) and 211H (podoplanin-negative) cells using anti-podoplanin antibody LpMab-17 (red). The nuclei were counterstained with DAPI (blue)
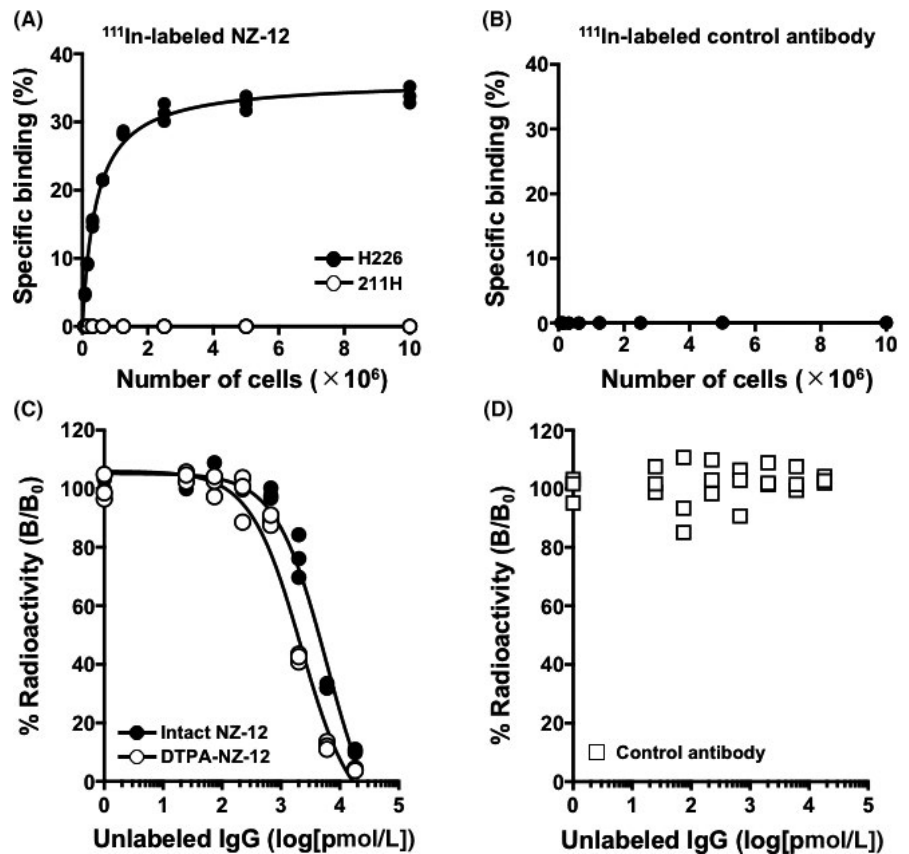
FIGURE 2 In vitro characterization of radiolabeled antibody NZ-12. A, Cell binding assay of ^{111}In-labeled NZ-12 with H226 (black circles) and 211H cells. (white circles). B, Cell binding assay of ^{111}In-labeled control antibody (IgG$_{1\lambda}$) with H226. C, Competitive inhibition assay for intact NZ-12 (black circles) and CHX-A''-DTPA-conjugated NZ-12 (white circles) with H226 cells. D, Competitive inhibition assay for control antibody (IgG$_{1\lambda}$)

Positive podoplanin staining on human specimens was found in 90% of all types of malignant mesothelioma specimens: 92% (12/13 cases) of epithelioid-type, 67% (2/3 cases) of sarcomatoid-type, and 100% (3/3 cases) of mixed-type.

3.7 | Treatment effects of external-beam radiation with X-rays in nude mice bearing H226 tumors

In mice irradiated with 25 and 50 Gy, H226 tumor volumes increased during the first 14 days and thereafter significantly decreased compared with the control (0 Gy) group ($P < .01$, Figure 7A). Tumor reduction was observed until day 28, and tumor volumes gradually increased thereafter. Grade of regrowth was more pronounced in the 25-Gy radiation group, and tumor size differed significantly between the 25-Gy and the 50-Gy groups from days 35 to 56 ($P < .01$ from days 35 to 45, $P < .05$ from days 49 to 56, Figure 7A). The radiation dose of 25 Gy corresponds to the estimated absorbed dose when injected with 3.70 MBq of ^{90}Y-labeled NZ-12, as mentioned above. No body weight reduction was observed in any of the groups (Figure 7B).

4 | DISCUSSION

Malignant mesothelioma is an aggressive tumor with a very poor prognosis.[1] More effective treatments must be developed to improve the prognosis. Malignant mesothelioma shows high expression levels

of podoplanin,[19] and the frequency of high podoplanin expression is similar to or higher than that of other mesothelioma-associated antigens such as calretinin, thrombomodulin, cytokeratin 5, WT1, and mesothelin.[28,38,39] Therefore, podoplanin is a promising immunological target for diagnosis and therapeutics in malignant mesothelioma. We previously developed a rat-human chimeric anti-podoplanin antibody, NZ-12, which has high specificity and high binding affinity for podoplanin expressed on mesothelioma cells.[30,31] In the present study, the potential of radiolabeled NZ-12 as a RIT agent was evaluated in a mesothelioma mouse model.

Immunofluorescence staining analysis of podoplanin expression in mesothelioma cell lines showed that high expression of podoplanin was observed on the membrane of H226 cells, but not on 211H cells, which is consistent with the findings of flow cytometric analysis in a previous study.[19] Thus, H226 as a positive control and 211H as a negative control were considered suitable for the subsequent in vitro studies. In vitro cell binding and competitive inhibition assays showed that ^{111}In-labeled NZ-12 bound specifically to podoplanin-expressing H226 cells with high affinity, and the affinity loss after the labeling procedures was limited, indicating that radiolabeled NZ-12 is acceptable for the following in vivo experiments.

Biodistribution studies in H226 tumor-bearing mice showed that tumor uptake of ^{111}In-labeled NZ-12 was significantly higher than that of ^{111}In-labeled control antibody. By replacing ^{111}In with a therapeutic radionuclide ^{90}Y, 3.70 MBq of ^{90}Y-labeled NZ-12 showed a stronger tumor growth suppression effect and prolonged survival

	1 h	Day 1	Day 2	Day 4	Day 7
Anti-podoplanin antibody NZ-12					
Blood	46.4 ± 3.8**	20.8 ± 2.8**	20.7 ± 1.1	14.9 ± 1.4**	11.6 ± 2.0
Brain	1.3 ± 0.4	0.7 ± 0.1	0.7 ± 0.1	0.4 ± 0.1	0.4 ± 0.1
Lung	14.0 ± 2.7	9.2 ± 0.8	9.4 ± 0.6	7.1 ± 1.5*	5.5 ± 0.9
Liver	10.8 ± 1.3**	6.7 ± 0.6	7.6 ± 0.4*	6.8 ± 0.8	5.3 ± 0.7
Spleen	6.6 ± 0.6**	6.0 ± 0.4**	6.3 ± 0.5**	5.3 ± 1.0	6.3 ± 0.6**
Pancreas	2.5 ± 0.5	2.3 ± 0.4	1.9 ± 0.2	1.6 ± 0.3*	1.3 ± 0.2
Stomach	1.7 ± 0.3	2.4 ± 0.6	1.9 ± 0.2	1.9 ± 0.4	1.5 ± 0.3
Intestine	3.8 ± 0.7	2.5 ± 0.3	2.3 ± 0.3	2.0 ± 0.3	1.5 ± 0.2
Kidney	11.4 ± 1.3	7.5 ± 0.8	7.3 ± 1.0	6.5 ± 0.8	4.7 ± 0.7
Muscle	0.7 ± 0.1	1.4 ± 0.1	1.3 ± 0.1**	1.2 ± 0.1**	1.0. ± 0.1
Bone	3.3 ± 0.7	2.5 ± 0.4	2.6 ± 0.3	2.2 ± 0.4	2.2 ± 0.6
H226 tumor	2.1 ± 0.3	12.0 ± 1.3**	18.0 ± 3.3**	22.4 ± 2.0**	23.2 ± 0.9**
Control antibody					
Blood	40.8 ± 2.4	25.3 ± 0.9	24.3 ± 1.6	20.4 ± 2.8	13.9 ± 1.2
Brain	1.2 ± 0.2	0.8 ± 0.2	0.8 ± 0.2	0.7 ± 0.2	0.6 ± 0.3
Lung	14.9 ± 1.3	10.2 ± 0.2	9.9 ± 0.7	9.2 ± 0.8	6.3 ± 0.6
Liver	7.7 ± 0.8	7.1 ± 0.6	5.8 ± 0.9	6.9 ± 0.9	6.6 ± 1.3
Spleen	4.6 ± 0.2	4.0 ± 0.3	4.5 ± 0.5	5.3 ± 0.7	4.2 ± 0.7
Pancreas	2.3 ± 0.2	2.4 ± 0.3	2.3 ± 0.2	2.2 ± 0.2	1.7 ± 0.4
Stomach	1.8 ± 0.2	2.4 ± 0.3	2.1 ± 0.4	2.2 ± 0.5	1.6 ± 0.5
Intestine	3.5 ± 0.5	2.3 ± 0.3	2.4 ± 0.4	2.2 ± 0.3	1.5 ± 0.1
Kidney	11.8 ± 1.1	7.7 ± 0.4	7.2 ± 1.0	6.5 ± 0.9	4.8 ± 0.4
Muscle	0.9 ± 0.1	1.7 ± 0.5	1.8 ± 0.3	1.8 ± 0.5	1.2 ± 0.1
Bone	3.0 ± 0.3	2.3 ± 0.2	2.3 ± 0.3	2.5 ± 0.3	1.6 ± 0.5
H226 tumor	1.8 ± 0.3	6.5 ± 0.5	7.0 ± 0.6	8.7 ± 2.0	9.0 ± 1.9

Data are expressed as percentage of injected dose per gram (% ID/g) and as mean ± SD.

**$P < .01$.

*$P < .05$, vs control antibody.

with statistically significant differences compared with giving intact NZ-12 and 3.70 MBq of ^{90}Y-labeled control antibody, whereas 1.85 MBq of ^{90}Y-labeled NZ-12 had no significant effect. Histological analysis showed an increase in necrotic foci and a reduced number of proliferating (Ki-67 positive) cells in H226 tumors treated with 3.70 MBq of ^{90}Y-labeled NZ-12. These histological alterations are frequently observed in tissues damaged by radiation.[40,41] Our findings suggest that ^{90}Y-labeled NZ-12 has the potential to treat malignant mesothelioma patients.
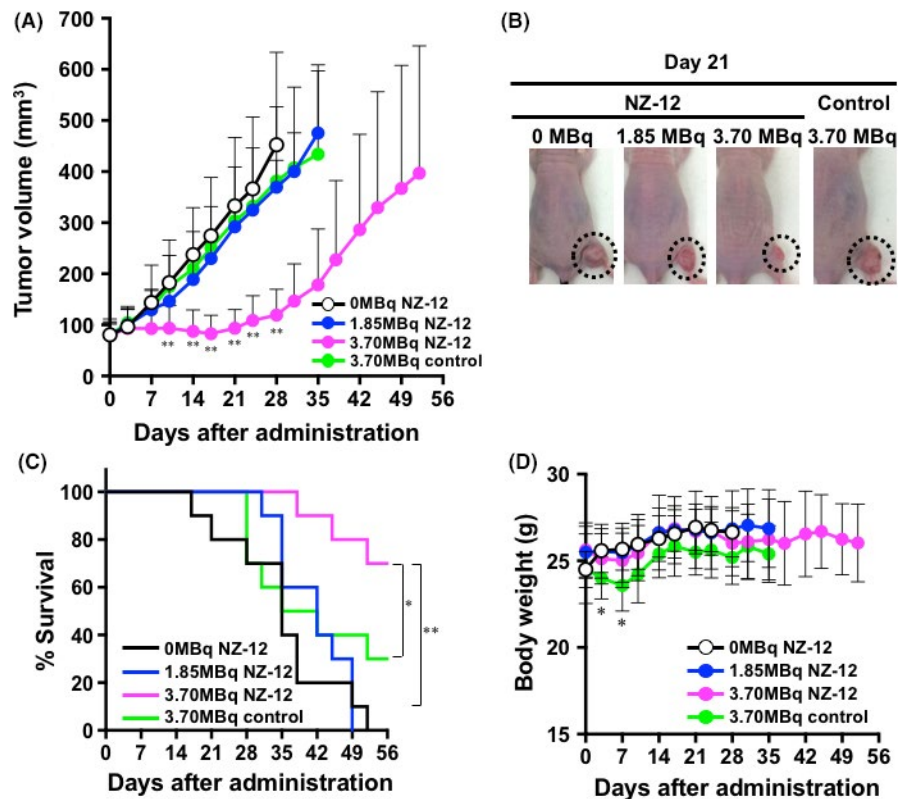
Radiation therapy for malignant mesothelioma patients is generally used as adjuvant therapy to prevent recurrences after surgical resection of early-stage mesothelioma and symptom palliation.[5] The standard dose of radiation therapy for preventing recurrences and symptom palliation is 21 Gy in three fractions or 20 Gy in four to five fractions according to the clinical practice guidelines for malignant mesothelioma.[5] Prophylactic irradiation may prolong the recurrence-free period, although it did not confer a statistically significant

TABLE 2 Estimated absorbed dose (Gy) of ^{90}Y-labeled antibody

	Anti-podoplanin antibody NZ-12		Control antibody
	1.85 MBq	3.70 MBq	3.70 MBq
Brain	0.5	1.1	1.3
Lung	7.2	14.4	15.9
Liver	5.9	11.8	10.6
Spleen	4.7	9.5	7.3
Pancreas	1.5	3.1	3.5
Stomach	1.5	3.1	3.4
Intestine	1.9	3.8	3.8
Kidney	6.0	12.0	12.0
Muscle	0.9	1.8	2.5
Bone	0.9	1.8	2.5
H226 tumor	12.4	24.8	10.6

FIGURE 3 Therapeutic efficacy of ^{90}Y-labeled antibodies in nude mice bearing H226 tumors. A, Tumor growth curves after injection with ^{90}Y-labeled NZ-12 and control antibody. Data indicate mean and SD (n = 10). **P < .01 vs 0 MBq of ^{90}Y-labeled NZ-12 (intact NZ-12 only). B, Representative images of mice at day 21 after injection with ^{90}Y-labeled NZ-12 and control antibody. Dashed circles indicate tumors. C, Kaplan-Meier survival curves based on the endpoints of tumor volume of 500 mm[3]. **P < .01, 0 MBq and 1.85 MBq of ^{90}Y-labeled NZ-12 vs 3.70 MBq of ^{90}Y-labeled NZ-12; *P < .05, 3.70 MBq of ^{90}Y-labeled control antibody vs 3.70 MBq of ^{90}Y-labeled NZ-12. D, Body weight changes after injection with ^{90}Y-labeled NZ-12 and control antibody. Data indicate mean and SD (n = 10). *P < .05 vs 0 MBq of ^{90}Y-labeled NZ-12

difference compared with unirradiated patients.[5] Palliative radiation therapy provides significant pain relief in approximately 50% of malignant mesothelioma patients.[5] In our dosimetry analysis, the absorbed dose to H226 tumors injected with 3.70 MBq of ^{90}Y-labeled NZ-12 was estimated to be 24.8 Gy, suggesting that it is potentially applicable for recurrence prevention and palliation.

The safety of RIT with ^{90}Y-labeled NZ-12 is important when considering clinical application. In the present study, giving 3.70 MBq of ^{90}Y-labeled NZ-12 induced no significant body weight loss and no visible adverse effects, such as diarrhea and dyspnea. Most mesothelioma cells spread into the diaphragm, chest wall, and mediastinum with an irregular shape and are close to critical structures such as the spinal cord, liver, esophagus, heart, and lungs.[42] Therefore, external-beam radiation to mesothelioma in the thorax and mediastinum has substantial technical limitations.[42,43] The most common toxicities in patients treated with external-beam radiation for thoracic cancer are symptomatic radiation pneumonitis,[44] and the mean dose to the lungs for 20% risk of radiation pneumonitis is 20 Gy.[44] The estimated absorbed dose in mouse lungs injected with 3.70 MBq of ^{90}Y-labeled NZ-12 was 14.4 Gy, suggesting a low risk of toxicity to the lungs in patients. The absorbed doses of the other organs are also considered tolerable because these absorbed doses are lower than the tolerance doses of those organs based on the findings of external-beam radiation studies.[45,46] This is supported by several previous studies using ^{90}Y-labeled antibodies, which showed no severe toxicities induced by similar absorbed doses.[10,47] Therefore, the risk of radiation-induced toxicity from RIT with ^{90}Y-labeled NZ-12 is expected to be low, although further dosimetry studies in malignant mesothelioma patients are required.

Giving 3.70 MBq of ^{90}Y-labeled NZ-12 delayed tumor growth in the H226 mesothelioma tumor model, whereas tumor volume reduction was observed in mice irradiated with X-rays of 25 Gy, which corresponds with the absorbed dose when injected with 3.70 MBq of ^{90}Y-labeled NZ-12, as mentioned above. Buras et al[48] reported that the antitumor effect by RIT is limited, especially in radioresistant tumors, compared with external-beam radiation therapy as a result of lower radiation dose rates of RIT. Similar findings were obtained in our previous RIT studies.[7,9] H226 is a radioresistant cell line[49] and, thus, the antitumor effect of RIT using ^{90}Y-labeled NZ-12 for H226 tumors was considered less effective than external-beam radiation therapy at the corresponding doses. However, ^{90}Y-labeled NZ-12 suppressed tumor growth and, therefore, further efforts as described below, may improve the therapeutic effect to achieve complete remission in malignant mesothelioma patients.

Currently, RIT is applied to hematological malignancies such as lymphoma, but not to solid tumors, because most solid tumors are more radioresistant.[50] To exert the full potential of RIT, radiolabeled antibodies must be specifically delivered in tumoricidal doses to tumors (eg, 30-50 Gy for radiosensitive tumors such as hematopoietic tumors, and 80-100 Gy for radioresistant tumors such as most solid tumors[51]), whereas radiation doses to healthy tissues must be limited.[50] Several potential strategies may improve the efficacy of RIT with ^{90}Y-labeled NZ-12. One approach is repeated dosing of ^{90}Y-labeled NZ-12, which can give H226 tumors approximately 25 Gy with no adverse effects, at least in mice. A simple calculation shows
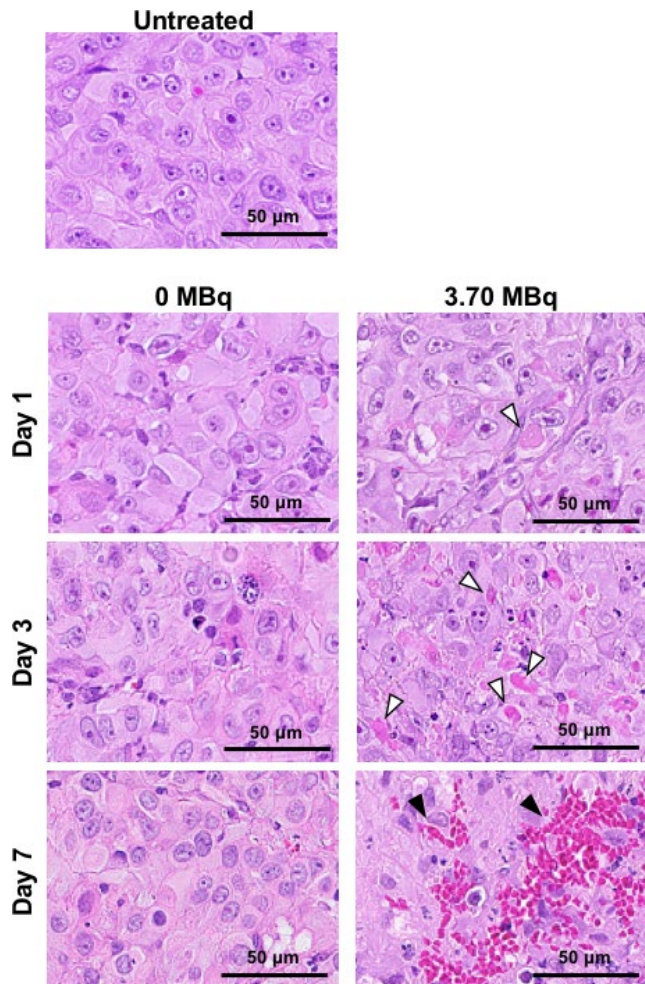
FIGURE 4 Histological analysis of H226 tumors after injection with 0 MBq (intact NZ-12 only) and 3.70 MBq of ^{90}Y-labeled NZ-12. Hematoxylin-and-eosin-stained sections of H226 tumors at days 1, 3, and 7 after injection. White arrowheads indicate necrosis and black arrowheads indicate hemorrhage

that a regimen of four repeated doses can provide approximately 100 Gy, which could be effective for solid tumors.[51] As mentioned above, RIT generally shows lower anticancer effects compared with external-beam radiation therapy and, thus, further cycles of dosing may be needed. Moreover, clinical studies for dosimetry in mesothelioma patients are required because the biodistribution of radiolabeled NZ-12 likely differs between mouse and human. In fact, the present immunohistochemical staining analysis showed higher podoplanin expression in human malignant mesothelioma specimens compared with H226 tumors, suggesting that ^{90}Y-labeled NZ-12 would likely accumulate more in tumors and deposit higher energy to tumors in patients than in H226 tumor xenografts. Second, a radiosensitizer could be combined with ^{90}Y-labeled NZ-12. Some chemotherapeutic agents such as pemetrexed and gemcitabine have radiosensitizing effects.[52,53] Pemetrexed is recommended as first-line chemotherapy for malignant mesothelioma[5] and is the first candidate as a radiosensitizer with RIT against mesothelioma. Third, repeated dosing with intact NZ-12 after RIT could enhance
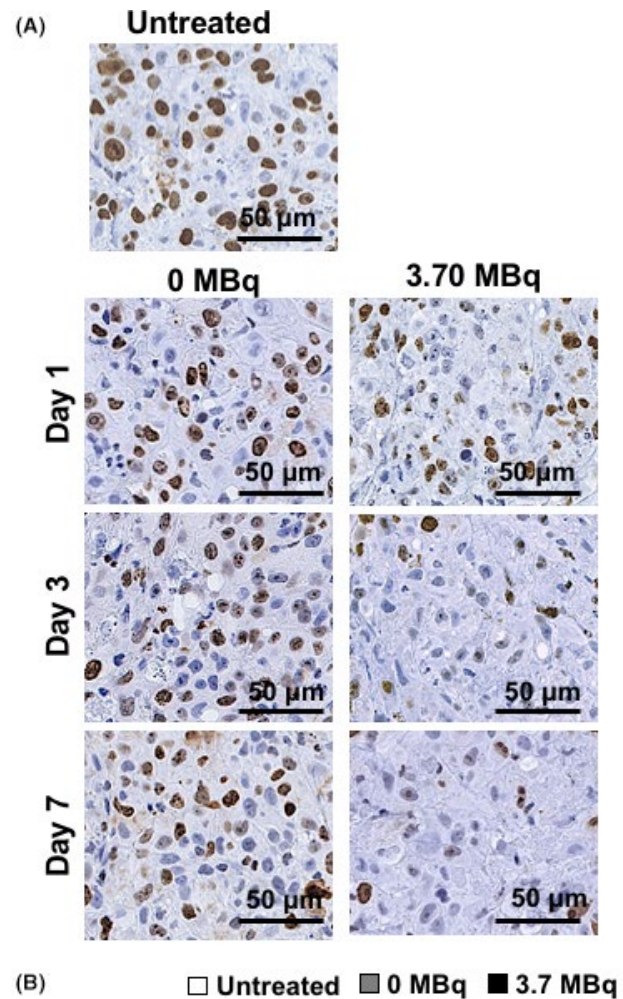

FIGURE 5 Tumor cell proliferation analysis by Ki-67 immunostaining. A, Ki-67-stained sections of H226 tumors at days 1, 3, and 7 after injection with 0 MBq (intact NZ-12 only) and 3.70 MBq of ^{90}Y-labeled NZ-12. B, Quantification of proliferating (Ki-67 positive) cells. Data are mean and SD. **$P < .01$, *$P < .05$

the therapeutic effect because NZ-12 is reported to induce potent antibody-dependent cellular cytotoxicity against podoplanin-expressing tumors.[30] NZ-12 is a chimeric antibody and is expected
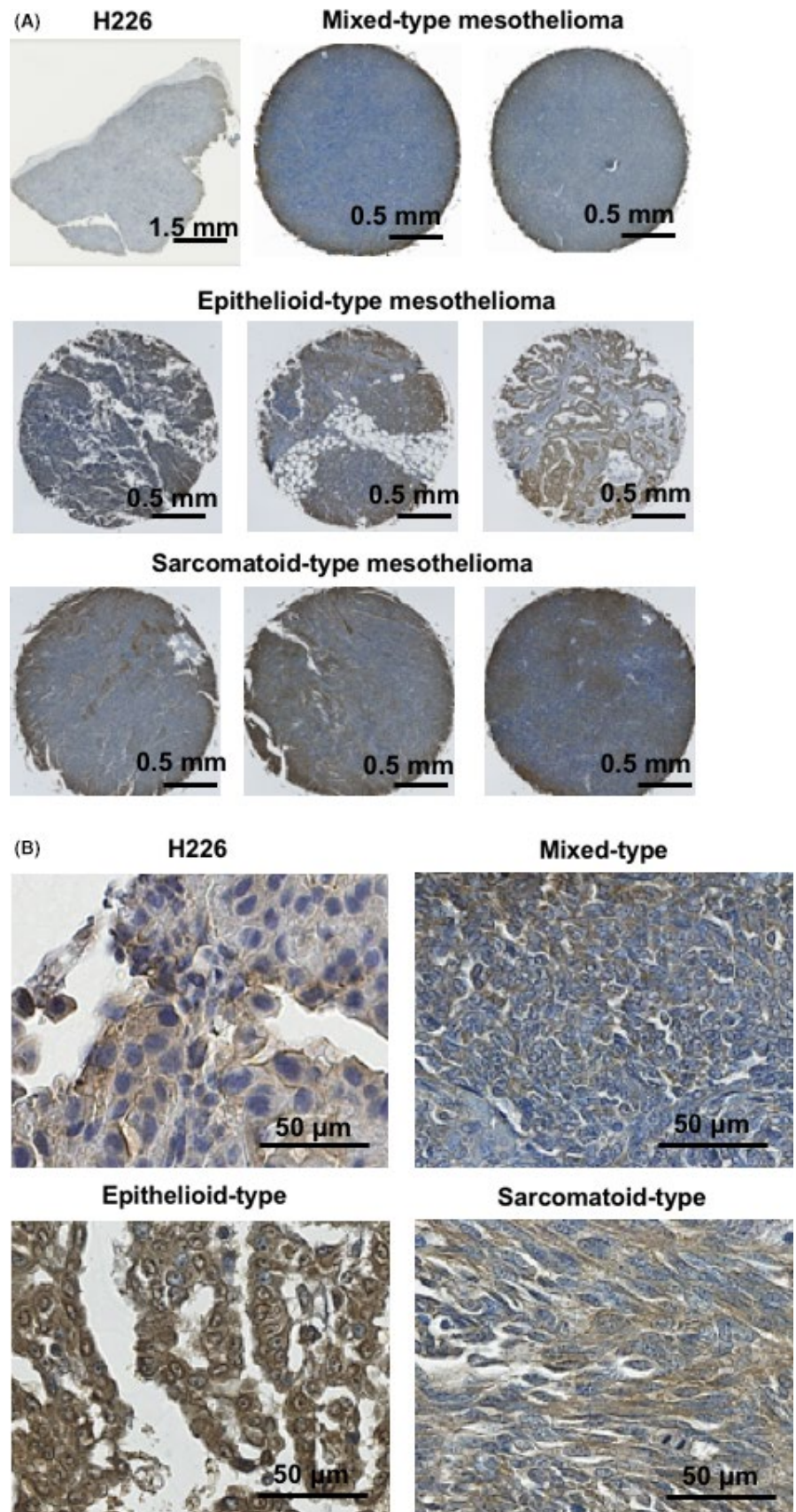
FIGURE 6 Podoplanin expression analysis in human mesothelioma specimens. A, Representative images of immunohistochemical staining with LpMab17. B, High magnification images of (A)

to have a low risk of immunogenicity, suggesting that NZ-12 is suitable for repeated dosing over a long period of time. Taken together, the triple combination of ^{90}Y-labeled NZ-12, pemetrexed, and intact NZ-12 has the potential to induce cytotoxic effects and suppress tumor growth for a long time. Further preclinical studies are needed to evaluate the efficacy and safety of these therapeutic options.
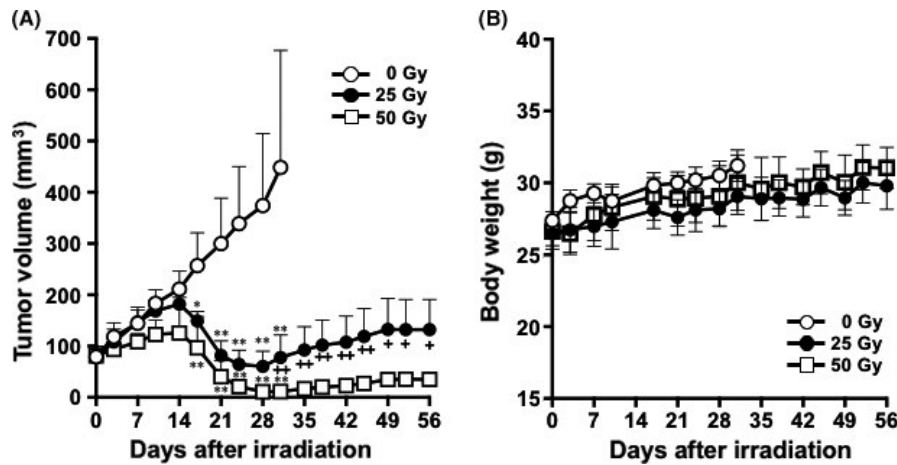
FIGURE 7 Therapeutic efficacy of external-beam radiation with X-rays in nude mice bearing H226 tumors. A, Tumor growth curves after irradiation with X-rays. Data indicate mean and SD (n = 5). $**P < .01$ and $*P < .05$ vs 0 Gy. $^{++}P < .01$ and $^{+}P < .05$, 25 Gy vs 50 Gy. B, Body weight changes after irradiation with X-rays. Data indicate mean and SD (n = 5)

TABLE 3 Summary of immunohistochemical analysis of podoplanin in human mesothelioma specimens

	Number	Positive (%)
Epithelioid	13	12 (92.3)
Sarcomatoid	3	2 (66.7)
Mixed	3	3 (100.0)
Total	19	17 (89.5)

Although the present study showed the potential of ^{90}Y-labeled NZ-12 as an RIT agent for the treatment of mesothelioma, there are some limitations. First, ^{90}Y-labeled NZ-12 delayed tumor growth, but further preclinical studies are needed to evaluate whether complete remission of malignant mesothelioma can be achieved, as mentioned above. Second, in the analysis of podoplanin expression, the number of human mesothelioma specimens analyzed for podoplanin expression was small and, thus, expression analyses using a larger number of specimens are needed. Third, further clinical studies are required to evaluate the dosimetry of radiolabeled NZ-12 in malignant mesothelioma patients for prediction of the therapeutic effects and safety.

In summary, giving 3.70 MBq of ^{90}Y-labeled anti-podoplanin antibody NZ-12 significantly suppressed tumor growth without body weight loss in a mesothelioma mouse model H226. Considering the higher expression levels of podoplanin in human malignant mesothelioma specimens compared with H226 tumors, RIT with ^{90}Y-labeled NZ-12 is a promising potential therapeutic option to provide greater clinical benefit to malignant mesothelioma patients.

CONFLICTS OF INTEREST

Authors declare no conflicts of interest for this article.

ORCID

Atsushi B. Tsuji https://orcid.org/0000-0003-2726-288X

Tsuneo Saga https://orcid.org/0000-0001-7801-9316

Yukinari Kato https://orcid.org/0000-0001-5385-8201

REFERENCES

1. Robinson BW, Lake RA. Advances in malignant mesothelioma. *N Engl J Med.* 2005;353(15):1591-1603.
2. Sterman DH, Albelda SM. Advances in the diagnosis, evaluation, and management of malignant pleural mesothelioma. *Respirology.* 2005;10(3):266-283.
3. Taioli E, Wolf AS, Camacho-Rivera M, et al. Determinants of survival in malignant pleural mesothelioma: a surveillance, epidemiology, and end results (SEER) study of 14,228 patients. *PLoS One.* 2015;10(12):e0145039.
4. Vogelzang NJ, Rusthoven JJ, Symanowski J, et al. Phase III study of pemetrexed in combination with cisplatin versus cisplatin alone in patients with malignant pleural mesothelioma. *J Clin Oncol.* 2003;21(14):2636-2644.
5. Kindler HL, Ismaila N, Armato S 3rd, et al. Treatment of malignant pleural mesothelioma: American Society of Clinical Oncology Clinical Practice Guideline. *J Clin Oncol.* 2018;36(13):1343-1373.
6. Kawashima H. Radioimmunotherapy: a specific treatment protocol for cancer by cytotoxic radioisotopes conjugated to antibodies. *ScientificWorldJournal.* 2014;2014: 492061.
7. Yoshida C, Tsuji AB, Sudo H, et al. Therapeutic efficacy of c-kit-targeted radioimmunotherapy using 90Y-labeled anti-c-kit antibodies in a mouse model of small cell lung cancer. *PLoS One.* 2013;8(3):e59248.

8. Fujiwara K, Koyama K, Suga K, et al. 90Y-labeled anti-ROBO1 monoclonal antibody exhibits antitumor activity against small cell lung cancer xenografts. *PLoS One*. 2015;10(5):e0125468.

9. Sugyo A, Tsuji AB, Sudo H, et al. Evaluation of efficacy of radioimmunotherapy with 90Y-labeled fully human anti-transferrin receptor monoclonal antibody in pancreatic cancer mouse models. *PLoS One*. 2015;10(4):e0123761.

10. Aung W, Tsuji AB, Sudo H, et al. Radioimmunotherapy of pancreatic cancer xenografts in nude mice using Y-90-labeled anti-alpha(6) beta(4) integrin antibody. *Oncotarget*. 2016;7(25):38835-38844.

11. Yudistiro R, Hanaoka H, Katsumata N, Yamaguchi A, Tsushima Y. Bevacizumab radioimmunotherapy (RIT) with accelerated blood clearance using the avidin chase. *Mol Pharm*. 2018;15(6):2165-2173.

12. Chandramohan V, Bao X, Kato KM, et al. Recombinant anti-podoplanin (NZ-1) immunotoxin for the treatment of malignant brain tumors. *Int J Cancer*. 2013;132(10):2339-2348.

13. Kato Y, Kaneko M, Sata M, Fujita N, Tsuruo T, Osawa M. Enhanced expression of Aggrus (T1alpha/podoplanin), a platelet-aggregation-inducing factor in lung squamous cell carcinoma. *Tumour Biol*. 2005;26(4):195-200.

14. Martín-Villar E, Scholl FG, Gamallo C, et al. Characterization of human PA2.26 antigen (T1alpha-2, podoplanin), a small membrane mucin induced in oral squamous cell carcinomas. *Int J Cancer*. 2005;113(6):899-910.

15. Schacht V, Dadras SS, Johnson LA, Jackson DG, Hong YK, Detmar M. Up-regulation of the lymphatic marker podoplanin, a mucin-type transmembrane glycoprotein, in human squamous cell carcinomas and germ cell tumors. *Am J Pathol*. 2005;166(3):913-921.

16. Xu Y, Ogose A, Kawashima H, et al. High-level expression of podoplanin in benign and malignant soft tissue tumors: immunohistochemical and quantitative real-time RT-PCR analysis. *Oncol Rep*. 2011;25(3):599-607.

17. Kato Y, Sasagawa I, Kaneko M, Osawa M, Fujita N, Tsuruo T. Aggrus: a diagnostic marker that distinguishes seminoma from embryonal carcinoma in testicular germ cell tumors. *Oncogene* 2004;23(52):8552-8556.

18. Kimura N, Kimura I. Podoplanin as a marker for mesothelioma. *Pathol Int*. 2005;55(2):83-86.

19. Abe S, Morita Y, Kaneko MK, et al. A novel targeting therapy of malignant mesothelioma using anti-podoplanin antibody. *J Immunol*. 2013;190(12):6239-6249.

20. Yuan P, Temam S, El-Naggar A, et al. Overexpression of podoplanin in oral cancer and its association with poor clinical outcome. *Cancer*. 2006;107(3):563-569.

21. Mishima K, Kato Y, Kaneko MK, Nishikawa R, Hirose T, Matsutani M. Increased expression of podoplanin in malignant astrocytic tumors as a novel molecular marker of malignant progression. *Acta Neuropathol*. 2006;111(5):483-488.

22. Hoshino A, Ishii G, Ito T, et al. Podoplanin-positive fibroblasts enhance lung adenocarcinoma tumor formation: podoplanin in fibroblast functions for tumor progression. *Cancer Res*. 2011;71(14):4769-4779.

23. Seki S, Fujiwara M, Matsuura M, et al. Prognostic value of podoplanin expression in oral squamous cell carcinoma–a regression model auxiliary to UICC classification. *Pathol Oncol Res*. 2014;20(3):521-528.

24. Nakazawa Y, Sato S, Naito M, et al. Tetraspanin family member CD9 inhibits Aggrus/podoplanin-induced platelet aggregation and suppresses pulmonary metastasis. *Blood*. 2008;112(5):1730-1739.

25. Breiteneder-Geleff S, Matsui K, Soleiman A, et al. Podoplanin, novel 43-kd membrane protein of glomerular epithelial cells, is down-regulated in puromycin nephrosis. *Am J Pathol*. 1997;151(4):1141-1152.

26. Rishi AK, Joyce-Brady M, Fisher J, et al. Cloning, characterization, and development expression of a rat lung alveolar type I cell gene in embryonic endodermal and neural derivatives. *Dev Biol*. 1995;167(1):294-306.

27. Breiteneder-Geleff S, Soleiman A, Kowalski H. Angiosarcomas express mixed endothelial phenotypes of blood and lymphatic capillaries - Podoplanin as a specific marker for lymphatic endothelium. *Am J Pathol*. 1999;154(2):385-394.

28. Ordonez NG. Podoplanin: a novel diagnostic immunohistochemical marker. *Adv Anat Pathol*. 2006;13(2):83-88.

29. Kato Y, Kaneko MK, Kuno A, et al. Inhibition of tumor cell-induced platelet aggregation using a novel anti-podoplanin antibody reacting with its platelet-aggregation-stimulating domain. *Biochem Biophys Res Comm*. 2006;349(4):1301-1307.

30. Abe S, Kaneko MK, Tsuchihashi Y, et al. Antitumor effect of novel anti-podoplanin antibody NZ-12 against malignant pleural mesothelioma in an orthotopic xenograft model. *Cancer Sci*. 2016;107(9):1198-1205.

31. Kaneko MK, Abe S, Ogasawara S, et al. Chimeric anti-human podoplanin antibody NZ-12 of lambda light chain exerts higher antibody-dependent cellular cytotoxicity and complement-dependent cytotoxicity compared with NZ-8 of kappa light chain. *Monoclon Antib Immunodiagn Immunother*. 2017;36(1):25-29.

32. Kassis AI. Therapeutic radionuclides: biophysical and radiobiologic principles. *Semin Nucl Med*. 2008;38(5):358-366.

33. Bhattacharyya S, Dixit M. Metallic radionuclides in the development of diagnostic and therapeutic radiopharmaceuticals. *Dalton Trans*. 2011;40(23):6112-6128.

34. Witzig TE, Gordon LI, Cabanillas F, et al. Randomized controlled trial of yttrium-90-labeled ibritumomab tiuxetan radioimmunotherapy versus rituximab immunotherapy for patients with relapsed or refractory low-grade, follicular, or transformed B-cell non-Hodgkin's lymphoma. *J Clin Oncol*. 2002;20(10):2453-2463.

35. Kato Y, Ogasawara S, Oki H, et al. Novel monoclonal antibody LpMab-17 developed by CasMab technology distinguishes human podoplanin from monkey podoplanin. *Monoclon Antib Immunodiagn Immunother*. 2016;35(2):109-116.

36. Sogawa C, Tsuji AB, Sudo H, et al. C-kit-targeted imaging of gastrointestinal stromal tumor using radiolabeled anti-c-kit monoclonal antibody in a mouse tumor model. *Nucl Med Biol*. 2010;37(2):179-187.

37. Eckerman KF, Endo A. *MIRD: radionuclide data and decay schemes*, 2nd edn. Reston, VA: The Society of Nuclear Medicine and Molecular Imaging; 2008.

38. Chirieac LR, Pinkus GS, Pinkus JL, Godleski J, Sugarbaker DJ, Corson JM. The immunohistochemical characterization of sarcomatoid malignant mesothelioma of the pleura. *Am J Cancer Res*. 2011;1(1):14-24.

39. Yaziji H, Battifora H, Barry TS, et al. Evaluation of 12 antibodies for distinguishing epithelioid mesothelioma from adenocarcinoma: identification of a three-antibody immunohistochemical panel with maximal sensitivity and specificity. *Mod Pathol*. 2006;19(4):514-523.

40. Baskar R, Lee KA, Yeo R, Yeoh KW. Cancer and radiation therapy: current advances and future directions. *Int J Med Sci*. 2012;9(3):193-199.

41. Yang J, Yue JB, Liu J, Yu JM. Repopulation of tumor cells during fractionated radiotherapy and detection methods (Review). *Oncol Lett*. 2014;7(6):1755-1760.

42. Ahamad A, Stevens CW, Smythe WR, et al. Intensity-modulated radiation therapy: a novel approach to the management of malignant pleural mesothelioma. *Int J Radiat Oncol Biol Phys*. 2003;55(3):768-775.

43. Ulger S, Cetin E, Catli S, Sarac H, Kilic D, Bora H. Intensity-modulated radiation therapy improves the target coverage over 3-D planning while meeting lung tolerance doses for all patients with malignant pleural mesothelioma. *Technol Cancer Res Treat*. 2017;16(3):332-338.

44. Emami B. Tolerance of normal tissue to therapeutic radiation. *Rep Radiother Oncol*. 2013;1(1):123-127.

45. Emami B, Lyman J, Brown A, et al. Tolerance of normal tissue to therapeutic irradiation. *Int J Radiat Oncol Biol Phys*. 1991;21(1):109-122.

46. Weinmann M, Becker G, Einsele H, Bamberg M. Clinical indications and biological mechanisms of splenic irradiation in chronic leukaemia and myeloproliferative disorders. *Radiother Oncol*. 2001;58(3):235-246.

47. Sugyo A, Tsuji AB, Sudo H, et al. Evaluation of Zr-89-labeled human anti-CD147 monoclonal antibody as a positron emission tomography probe in a mouse model of pancreatic cancer. *PLoS One*. 2013;8(4):e61230.

48. Buras RR, Wong JY, Kuhn JA, et al. Comparison of radioimmunotherapy and external beam radiotherapy in colon cancer xenografts. *Int J Radiat Oncol Biol Phys*. 1993;25(3):473-479.

49. Carmichael J, Degraff WG, Gamson J, et al. Radiation sensitivity of human-lung cancer cell-lines. *Eur J Cancer Clin Oncol*. 1989;25(3):527-534.

50. Larson SM, Carrasquillo JA, Cheung NK, Press OW. Radioimmunotherapy of human tumours. *Nat Rev Cancer*. 2015;15(6):347-360.

51. Chatal JF, Davodeau F, Cherel M, Barbet J. Different ways to improve the clinical effectiveness of radioimmunotherapy in solid tumors. *J Cancer Res Ther*. 2009;5:36-40.

52. Wouters A, Pauwels B, Lardon F. In vitro study on the schedule-dependency of the interaction between pemetrexed, gemcitabine and irradiation in non-small cell lung cancer and head and neck cancer cells. *BMC Cancer*. 2010;10:441.

53. Oleinick NL, Biswas T, Patel R, et al. Radiosensitization of non-small-cell lung cancer cells and xenografts by the interactive effects of pemetrexed and methoxyamine. *Radiother Oncol*. 2016;121(2):335-341.